THESIS FOR THE DEGREE OF DOCTOR OF PHILOSOPHY

Designing Self-Assembling Structures of Particles and Cells

OSKAR LINDGREN

Department of Energy and Environment
Division of Physical Resource Theory, Complex Systems Group
CHALMERS UNIVERSITY OF TECHNOLOGY
Göteborg, Sweden 2015

Designing Self-Assembling Structures of Particles and Cells
OSKAR LINDGREN

THESIS FOR THE DEGREE OF DOCTOR OF PHILOSOPHY

Department of Energy and Environment
Division of Physical Resource Theory
Complex Systems Group
CHALMERS UNIVERSITY OF TECHNOLOGY
SE-412 96 Göteborg
Sweden
www.chalmers.se
Tel. +46-(0)31 772 1000

Author email: `oskar.lindgren@chalmers.se`

Cover: Hierarchical self-assembly of patchy colloids in Monte Carlo simulations. Surface particles with simple isotropic interactions self-assembles into functional patterns that in turn causes the coated colloids to self-assemble into cubic aggregates (b). The interactions that cause the self-assembly was derived using an energy spectrum, the Fourier transform of the interactions (a).

Printed by Reproservice
Göteborg, Sweden 2015

Designing Self-Assembling Structures of Particles and Cells

OSKAR LINDGREN
Department of Energy and Environment, Chalmers University of Technology

Abstract

This thesis presents a series of theoretical results on self-assembly. It includes explaining why certain two-dimensional patterns are universal, i.e., why they are expected to emerge for in aggregating two-dimensional particle systems. The thesis also outlines methods for deriving isotropic interaction potentials causing self-assembly of crystal lattices, and principles for understanding and designing self-assembling functional surface patterns, which in turn leads us to the design of hierarchical self-assembly of patchy particles. Inspired by biological systems, I also explore the possibility of using bio-inspired cellular growth to design self-assembling cellular structures from scratch.

Keywords: Self-assembly, patterns, colloids, isotropic interactions, chiral surfaces, patchy particles, hierarchical self-assembly, morphogenesis

List of publications

I. Erik Edlund, Oskar Lindgren and Martin Nilsson Jacobi, "Novel Self-Assembled Morphologies from Isotropic Interactions", *Physical Review Letters* **107**, 085501 (2011).
My contribution is the morphological alphabet and matching the outcomes of particle simulations to the alphabet. Writing the article was a joint effort. While I initially found the patterns in lattice simulations, Martin was the one who recognised them as spherical Bessel functions.

II. Erik Edlund, Oskar Lindgren and Martin Nilsson Jacobi, "Designing Isotropic Interactions for Self-Assembly of Complex Lattices", *Physical Review Letters* **107**, 085503 (2011).
I wrote the program and performed the simulations of the self-assembling lattices. I also figured out the requirements that guarantee that a target lattice is the ground state. Writing the article was a joint effort.

III. Erik Edlund, Oskar Lindgren and Martin Nilsson Jacobi, "Chiral Surfaces Self-Assembling in One-Component Systems with Isotropic Interactions", *Physical Review Letters* **108**, 165502 (2012).
I wrote the program and performed the simulations of the self-assembling lattices. I made, and explained the behaviour of, the phase diagram. Writing the article was a joint effort.

IV. Erik Edlund, Oskar Lindgren and Martin Nilsson Jacobi, "Using the uncertainty principle to design simple interactions for targeted self-assembly", *Journal of Chemical Physics* **108**, 024107 (2013).
I derived interaction potentials and performed simulations. Martin figured out the justification for the optimal smoothing of the interaction functions. Writing the article was a joint effort.

V. Erik Edlund, Oskar Lindgren and Martin Nilsson Jacobi, "Predicting self-assembled patterns on spheres with multicomponent coatings", *Soft Matter* **10**, 2955-2960 (2014).
See article six.

VI. Erik Edlund, Oskar Lindgren and Martin Nilsson Jacobi, "A design path for hierarchical self-assembly of patchy colloids", *Soft Matter*, DOI: 10.1039/C5SM00596E (2015). Articles five and six were at fist supposed to be one article. While all of us worked on how to generalise the theory underlying the previous articles to multiple particle types, Erik figured out how to use the stoichiometry and the spectral minima to figure out the ground state. While Erik simulated and explained the typical stripe/spot combinations that article five focuses on, I figured out how to obtain the patterns that are part of the hierarchical self-assemblies presented in this article and simulated these. I did some writing and illustrations and confirmed Erik's work for article five–but I led and did most of the work on article six, including writing most of it.

Acknowledgements

First I would like to thank you, colleagues at Physical Resource Theory. Thank you Martin, Kristian and Erik for being such talented and helpful colleagues and friends and for making our workplace such a welcoming and collaborative environment to grow in. I feel much more like a scientist now than when I started my doctoral studies. Thank you Mamma and Pappa, Johan, Sofia and John, Hannes and Emily, Jakob, Ivar, Gustav and Wen, and other friends and relatives. I look forward to spending much more time with you this spring and the coming summer! I give my greatest thanks, and all my love to you Mikaela, for the times you kept me going and to the son you have given us, Isak. Isak, you are wonderful.

Göteborg, May 2015
Oskar Lindgren

Contents

Chapter 1

Introduction

Many technological advancements relies on breakthroughs in material science. In fact, the components used in modern consumer electronics have complex structures on the nano- and micro-scale. Examples include cell phone batteries [1], optical circuits [2] and meta materials for limit breaking optics and signalling [3]. Material science invents more and more complicated structures to satiate the demand from industry, but traditional production methods become more difficult. Self-assembly has been suggested as an easily scalable alternative to conventional manufacturing. Instead of arranging the constituent particles by external influence like etching or by directed forces, we design the particles to arrange spontaneously into desired structures by free energy minimisation. However, for self-assembly to compete with other production methods we need methods for designing constituents that self-assembles into a requested structure. This is a difficult problem. While significant progress has been made on the experimental side of self-assembly, there is a dearth of theoretical results.

Carbon is a prime example of the role a material's structure can have on its properties. Arranged in a face-centered cubic crystal structure (diamond) carbon's hardness and thermal conductivity rank among the highest of all known bulk materials while graphite, weakly bound carbon flakes, is used to write with due to the ease with which these flakes break off and stick to surfaces. Graphene, a single graphite flake on the other hand, has singular electronic and mechanical properties and carbon nanotubes, rolled up graphene, could in the future anchor asteroids to the earth and make elevators a viable way to reach space. At larger length scales we find meta materials designed to exhibit properties not found in nature, for example materials with negative refractive indices, which could greatly increase optical resolution beyond what is possible with conventional lenses [4].

From a purely scientific point of view, studying self-assembly is interesting– emergence of order is a fundamental concept in biology. Indeed life could be considered the most complex form of self-assembly, but pattern formation is common in physical and chemical systems as well. A theoretical basis for self-assembly and emergence is important for understanding patterns and symmetry in nature and why some shapes are more common than others.

1.1 Universality, comprehensibility and analytical models

One key issue with using self-assembly to grow materials or build small components is to find out how the constituents should interact in order to assemble into the desired structures. There are several examples of experimental research and simulations on self-assembly [5–7], but little progress has been made on the theoretical side on broadly applicable principles and methods for designing which pattern that self-assembles. And not without reason–predicting and designing targeted self-assembly is difficult. Our starting point should be a model both broad enough to describe many different interactions accurately, but also compact in its formulation so that it is easy to treat mathematically. Consider a particle system where the contributions to the free energy from each particle pair only depend on the distance between the two particles. The distance dependence is described by an interaction (or effective interaction) potential, the shape of the potentials represents how the interactions between colloidal- or nano particles can be tuned in order to achieve self-assembly. The free energy of this system as a function of the particle positions will be characterised by several local minima in many dimensions. If we want to find a combination of interactions in the entire parameter space (if any such combination exists at all) that causes a desired particle configuration to have the lowest free energy or successfully deduce which configuration has the lowest free energy from the interaction potential, we must be able to address this problem. This is especially true in colloidal physics where there are numerous ways to influence how the colloids interacts, i.e., a large search space of complicated interactions [8–10].

Approximate models of self-assembling systems, simplified to such a degree that analytical tools are applicable but where the system still exhibits non-trivial behaviour, can be of use to understand and guide design of self-assembly in the modelled system. This is the central theme of this thesis. I describe the development of designed self-assembly of increasingly complicated patterns, with a focus on results that fall into one of three broad categories:

1. *Universality*: We want to understand why some patterns are repeatedly found in nature. If new classes of interactions were made available in, for example, chemical or biological systems, should we expect new types of patterns? Universal patterns can be expected to be obtained more easily, since the cause of their formation is independent of the particulars of the interactions in a given system. It is clear that the question of whether or not a pattern is universal is most easily answered by doing surveys, but to understand why some patterns are more common, a theoretical model of some sort is helpful [11]. Paper I addresses universal aggregate structures in large particle systems with long range interactions. Both the predictions in Paper V and the design path in Paper VI is based on universal patterns in a spherical geometry.

2. *Predictability*: If the pattern formation in a system can be intuitively or mathematically linked to mechanisms of the self-assembly process, it could be of great use for designing other self-assembling patterns. Paper VI gives examples of hierarchical self-assembly of patchy colloids, where the direction in which patches should connect can be chosen in an intuitive manner due to a high degree of control over the self-assembling patches themselves. The draft paper in Appendix. 6 explores if the growth mechanisms behind shells and protrusions in a cell model are intuitive.

3. *Exactly solvable models*: If we desire a target structure, how do we design interactions that cause self-assembly into that structure? This has previously been addressed using trial and error schemes [12]. But as the search space of possible interactions becomes larger, and we desire more complex target structures, the use of exactly solvable models for the self-assembly can greatly reduce and sometimes eliminate the need for trial and error. Paper I through Paper VI are based on Fourier representations of lattices or particles and draw conclusions about the energy and structural features of the ground state by using analytically tractable models. This enables us to design interaction potentials and find model parameters that cause a wide range of patterns in both two-dimensional and three-dimensional systems to self-assemble.

1.2 Overview of the thesis

Chapter 2 discusses recent advances in targeted self-assembly of particles into crystalline structures, from previous trial and error schemes to experimental feasibility, energy minimisation and the analytical design principle developed in Paper II through Paper IV. The principle is based on expressing the energy of a set of particles interacting with isotropic interactions in reciprocal space. By treating the particles not as a set of coordinates but as weight factors for Fourier modes, it is possible to limit how low the free energy can be for any particle configuration. This is done by imposing constraints on which Fourier modes are allowed, and translating the constraints to the interaction potential by Fourier transformation. By extension, it is possible to ensure that a target crystal structure will be the unique ground state, i.e. that there are no other particle configuration more energetically favourable for the designed interaction potential. The design principle has been demonstrated for two- and three-dimensional crystal structures of various complexity including chiral structures.

Fourier analysis can also be used to infer large scale features of the ground state configuration in our model system. In chapter 3 this is used to predict and explain the alphabet of universal two-dimensional aggregate patterns presented in Paper I. These patterns are closely tied to Fourier-Bessel series which more elegantly describes symmetrical patterns around a nucleation point. The spherical model can be generalised to other geometries like the surface of a sphere and to include multiple particle types, each with different inter-particle interactions. When taking into account constraints set by a fixed stoichiometry, it is possible to predict the ground state of alkanethiol molecules adsorbed on nanoparticles.

Chapter 4 gives examples of hierarchical self-assembly. One is in a model of nanoparticles coated with different types of molecules capable of self-assembling into different surface patterns. By combining the methods and principles developed in the previous chapters, we describe how to find model parameters that customises the surface pattern. These can in turn be designed so that the patchy nanoparticles self-assemble into geometrical structures, due to how the patches of the surface pattern are arranged. Different types of structures can be made: strings, membranes, lattices or aggregates. Another example of hierarchical self-assembly is organic life. Biological systems self-assembles on a wide range of scales, from protein folding to the growth and reproduction of individuals. The second part of chapter 4 explores the relationship between a simple mechanism for cell growth and the patterns cells grow in, with the goal of creating a similar set of tools used in the other articles for designing and predicting the shape of artificial multicellular life.

Chapter 5 gives a short summary of the main findings of each article. Chapter 6 gives a summary of the thesis and outlines the progress on our collaborative work on in vitro nano particle sedimentation, and how to combine the Fourier approach used successfully for nanoparticle self-assembly models with a more accurate version of the cellular model in order to design more complicated growth patterns.

Chapter 2

Self-assembly

Self-assembly is when components arrange themselves into a target pattern based on how they interact with each other. This could mean designed building blocks that for example need to be oriented in a desired way to connect or components repelling each other if they are not supposed to be adjacent. Self-assembly is in stark contrast to fabricating from blueprints where every piece has to be placed into its designated position by external guidance.

Broadly speaking, there are two approaches to designing self-assembly. Either you consider the time evolution of a system. The design consists of influencing the system in order to steer its steepest descent path through the energy landscape into a desired meta stable state. Examples can be found in applied chemistry where e.g. porosity and structure are often obtained by trapping a system undergoing spinodal decomposition before it has time to fully relax into its ground state, or by adding components one type at a time. Making small changes to a well studied process in order to perturb the end state is relatively easy, but obtaining completely new behaviour without resorting to trial and error is not since that would require a good description of large part of the energy landscape.

An alternative approach is to design the interactions among the constituents of a system so that the desired configuration is the ground state. The idea is that eventually the system will find the global ground state and that local minima in the energy landscape are avoided by annealing. The benefit to this is that only one or a few extreme points in the energy landscape have to be considered. This can make both design and predictions easier since one can take advantage of properties of the energy landscape that might only be true at those positions. Paper I through Paper VI focuses on this approach.

Biological processes, of which the self-assembly in the draft paper, Appendix. 6, is an example, could be considered to be hierarchies of self-assembling or self-organising systems. On the molecular scale there is for example DNA and protein-folding that reliably form the most energetically favourable configuration. Conversely DNA origami, a recent principle for sequencing DNA strands that fold into desired patterns only concerns itself with designing the ground state [13]. At the opposite side of the spectrum we find cellular morphogenesis, the catch-all term for how organisms develop their shape. At a chemical level these processes are of course described by thermodynamics and change towards lower chemical potential. But the behaviour of cells are separated from the chemical processes by hierarchies of self-assembly, making it much more reasonable to describe cellular morphogenesis using a mechanistic model where cells behave differently depending on surroundings and history. After all, if you scramble an organism on any level, it will not rearrange into the same configuration from temperature annealing. As a side note, there are examples of pattern regulation in nature that behaves similarly to a system seeking a local energy minima, like the segment sequencing of insect legs [14] or the extreme generative capabilities of some planarians [15].

2.1 Configuration energy in reciprocal space

Most of the thesis will concern self-assembly in systems where, at some level, the interactions between the components are isotropic. The energy of a system of n particles with positions $\{\mathbf{r}_i\}_{i=1}^{n}$ interacting with an isotropic, pairwise additive potential $V(r)$ can be expressed as the sum of the contributions from all particle pairs

$$E = \frac{1}{2}\sum_{i\neq j} V(|\mathbf{r}_i - \mathbf{r}_j|). \tag{2.1}$$

Trying to find an analytic expression for the configuration that minimises the energy is very difficult, even for very simple interaction potentials $V(r)$. For example the ground state for the Lennard-Jones potential is only proven for one-dimensional systems despite the fact that the Lennard-Jones potential only has a single minimum at short ranges and is a simple rational function [16]. This could make it seem even more difficult to design the interaction potential so that the target particle configuration is *guaranteed* to be the ground state. After all finding out the (approximate) ground state is easily done via a simulated annealing of the particle configuration, but even if one designs a potential that causes the target configuration to have low energy, there could still be another configuration with even lower energy. Since a local minimum in the interaction potential will cause the particles to prefer that distance to each other, it should be easier to design self-assembly of structures where a few distances repeats many times. Repeating distances is the defining property for crystal structures and it turns out that when crystalline patterns are expressed in terms of Fourier series (the reciprocal lattice) it's possible to compare them energy-wise to any conceivable particle configuration.

Fourier analysis is applied in solid-state physics to treat properties of ordered groups of particles. To express a particle configuration in terms of Fourier modes we need a density function describing how particles are distributed in space, with Dirac delta functions (in d dimensions) centred at each particles' position.

$$\rho(\mathbf{r}) = \sum_{i=1}^{n} \delta_d(\mathbf{r} - \mathbf{r}_i) \tag{2.2}$$

$$E = \int \mathbf{dr}_1 \mathbf{dr}_2 \rho(\mathbf{r}_1)\rho(\mathbf{r}_2)V(|\mathbf{r}_1 - \mathbf{r}_2|). \tag{2.3}$$

Expressing the energy in terms of the reciprocal lattice, the Fourier transform of the particle density function gives

$$\rho(\mathbf{r}) = \frac{1}{\sqrt{2\pi}} \int \mathrm{d}\mathbf{k}\hat{\rho}(\mathbf{r})e^{i\mathbf{kr}} \tag{2.4}$$

$$\hat{\rho}(\mathbf{k}) = \frac{1}{\sqrt{2\pi}} \int \mathrm{d}\mathbf{r}\rho(\mathbf{r})e^{-i\mathbf{kr}} \tag{2.5}$$

$$E = \frac{1}{2\pi} \int \mathrm{d}\mathbf{r}_1 \mathrm{d}\mathbf{r}_2 \int \mathrm{d}\mathbf{k}_1 \hat{\rho}(\mathbf{k}_1)e^{i\mathbf{k}_1\mathbf{r}_1}\rho(\mathbf{r}_2)V(|\mathbf{r}_1 - \mathbf{r}_2|). \tag{2.6}$$

$$\tag{2.7}$$

After changing the order of integration and substituting $\mathbf{r}_1 - \mathbf{r}_2 = \mathbf{r}$ and taking advantage of the isotropy of $V(r)$ we get

$$E = \int \mathrm{d}\mathbf{k}_1 \underbrace{\frac{1}{\sqrt{2\pi}} \int \mathrm{d}\mathbf{r}_2 e^{i\mathbf{k}_1\mathbf{r}_2}\rho(\mathbf{r}_2)}_{\hat{\rho}^*(\mathbf{k}_1)} \hat{\rho}(\mathbf{k}_1) \int \mathrm{d}\mathbf{r}V(|\mathbf{r}|)e^{i\mathbf{k}_1\mathbf{r}} \tag{2.8}$$

$$= \int \mathrm{d}\mathbf{k}\hat{\rho}^*(\mathbf{k})\hat{\rho}(\mathbf{k}) \int \mathrm{d}\mathbf{r}V(|\mathbf{r}|)e^{i\mathbf{kr}}. \tag{2.9}$$

Here we use the fact that the density function $\rho(\mathbf{r})$ is real and thus equal to its complex conjugate in order to switch between the Fourier transform and its inverse. By switching to reciprocal space we have exchanged the double integral for a quadratic term $|\hat{\rho}(\mathbf{k})|^2$. The energy is now expressed in terms of the Fourier transform of the particle configuration, which defines the periodicities present among the particles, and an energy spectrum

$$E = \int \mathrm{d}\mathbf{k} |\hat{\rho}(\mathbf{k})|^2 \hat{V}(k).. \tag{2.10}$$

The energy spectrum is the Fourier transform of the interaction potential and describes the energy associated with different periodicities

$$\hat{V}(k) = \int \mathrm{d}\mathbf{r} V(|\mathbf{r}|) e^{i\mathbf{k}\mathbf{r}}. \tag{2.11}$$

2.2 Targeted self-assembly of lattices

To understand how Eq. 2.10 can be used to design interactions that cause self-assembly of target crystal structures, one must first turn to solid-state physics and the description of crystal structures in Fourier space. A crystal is defined by its Bravais lattice and basis. The lattice describes the periodicity of the crystal and is given by linearly independent vectors $\{\mathbf{a}_i\}_{i=1}^{d}$ for which a translation will leave the d dimensional crystal structure invariant. The crystal lattice is the set of vertices generated by all linear combinations of the lattice vectors using integer coefficients. The basis describes how particles are arranged around every vertex so that the positions of all particles (without counting any particle twice) can be written as $\{\mathbf{p}_j + \sum_{i=1}^{d} \alpha_i \mathbf{a}_i\}_{\alpha_i \in \mathbb{Z}}$ and $\{\mathbf{p}_j\}_{j=1}^{m}$ is the lattice basis consisting of m particles (see Fig. 2.4 for an illustration). The density function can only be comprised of Fourier modes that are left invariant under the same translations as above. The Fourier transform of the density function will be another Bravais lattice called the reciprocal lattice $\mathbf{G}$, spanned by lattice vectors $\mathbf{g}_i$ satisfying

$$\mathbf{g}_i \mathbf{a}_j = 2\pi \delta_{ij}. \tag{2.12}$$

It is easy to check that a translation along any lattice vector will leave the Fourier modes of the reciprocal lattice vectors $\mathbf{g}_i$ unchanged

$$e^{i\mathbf{g}_j(\mathbf{r}+\mathbf{a}_k)} = e^{i\mathbf{g}_j\mathbf{r}} e^{i\mathbf{g}_j\mathbf{a}_k} = e^{i\mathbf{g}_j\mathbf{r}} e^{i2\pi\delta_{jk}} = e^{i\mathbf{g}_j\mathbf{r}}. \tag{2.13}$$

Since every Fourier mode in the reciprocal lattice can be written as a product of the $\mathbf{g}_i$ modes and each term is left invariant under a translation, this holds for all Fourier modes in the reciprocal lattice.

Consider an energy spectrum $\widehat{V}(k)$, Eq. 2.11, that is positive. Due to the quadratic dependence in Eq. 2.10 any density function would describe a configuration with positive or zero energy. By choosing $\widehat{V}(k) \geq 0$, with zeros only at the radii k where the reciprocal lattice has support, it is possible to guarantee that the target structure is a ground state with zero energy. Note that the ground state will be degenerate, which we will come back to soon. Non-crystalline structures will have small positive energy contributions from all regions of the spectrum and non space-filling structures will have contributions from (among other) the low k part of the spectrum, both resulting in positive energy levels. Could there be other Bravais lattices that compete with the target lattice? The energy spectrum directly excludes Bravais lattices with different distances between vertices (in reciprocal space) than in the target, $|\mathbf{G}|$, this ensures that the lattice vector norms are correct. If the energy spectrum covers a sufficient amount of vertices in reciprocal space the Bravais lattice will be uniquely determined by triangulation.

This principle allows us to design energy spectra, and by inverse Fourier transform we obtain interaction potentials that cause self-assembly of Bravais lattices. Since the basis doesn't change the periodicity of the crystal structure, it will have no effect on the support of $\hat{\rho}$. This means that any crystal structure with the correct Bravais lattice will have zero energy, independent of the basis, and causes the ground state degeneracy mentioned before. In order to design self-assembly of crystal structures with multiple particles in the basis, we need to energetically differentiate the target from alternative bases. This can be done by perturbing the energy spectra, making the desired lattice basis the energetically favoured one. Consider the lattice basis's influence on the energy in Eq. 2.10. By Fourier-transforming the density function we get a complex exponential for each vertex in the Bravais lattice, but since the basis is repeated at each such vertex we can separate the influence of the basis from the influence of the lattice

$$\hat{\rho}(\mathbf{k}) = \int \mathrm{d}\mathbf{r}\rho(\mathbf{r})e^{i\mathbf{kr}} = \underbrace{\left(\sum_{j=1}^{m} e^{i\mathbf{k}\mathbf{p}_j}\right)}_{f(\mathbf{k})} \sum_{\alpha_i\in\mathbb{Z}} e^{i\mathbf{k}(\sum_{i=1}^{d}\alpha_i\mathbf{a}_i)}. \tag{2.14}$$

The lattice terms are simply delta functions coinciding with the vertices of the reciprocal lattice, but the scaling factor in front stemming from the structure of the basis will differ for different wave vectors. In solid state physics this term is called the crystal structure factor $f(\mathbf{k})$ and influences how waves propagate through a crystal. The energy for a crystal structure becomes

$$E = \sum_{\mathbf{k}\in\mathbf{G}} |f(\mathbf{k})|^2 \hat{V}(k). \tag{2.15}$$

Evident from Eq. 2.14 is that the norm of the scaling factor has an upper bound equal to the number of particles in the basis. A small negative perturbation of the energy spectra at a k value where the structure factors equal the upper bound can guarantee that the relative positions of the particles in the basis are correct. This condition is generally reached when the crystal structure can be thought of as a Bravais lattice with vacancies, like the Kagome or honeycomb structure or in three dimensions, the diamond structure. In the Kagome lattice, for example, a negative perturbation at the third zero in the energy spectrum guarantees that the Kagome basis has the lowest energy, Fig. 2.1. There are four $\mathbf{r}$ values that maximise these $f(\mathbf{k})$ within the unit cell, and the basis consists of three particles, but no matter which of the sites are empty, the crystal lattice will still be a Kagome lattice. For more complicated crystal lattices, multiple negative perturbations where the structure factor maxes out and positive perturbations where it cancels out might be necessary to uniquely select for the target crystal structure. The perturbation does not necessarily have to reside in the energy spectrum either. If the target configuration is a lattice where the nearest neighbouring particles are at a set distance from each other the perturbation might be done on the derived interaction potential instead with a negative perturbation at the nearest neighbour distance, although the analytical argument for why it is a ground state is lost.

Previous work on designing isotropic interaction potentials for targeted self-assembly has focused on minimising energy in real space by matching the interaction potential [17] to the pair correlation function of a series of contesting crystal structures. The advantage of designing the energy spectrum to match the reciprocal lattice instead of the interaction potential to match the pair correlation function is that the lattice structure is completely encoded in the low k region, the information stored in the high k region of the reciprocal space is just to better resolve the particles, as seen in Fig. 2.1. Another argument is that in reciprocal space the lattice structure and the basis are decoupled. The support of $\hat{\rho}(\mathbf{k})$ defines the Bravais lattice, and its amplitude defines the basis. If one designs an interaction potential using the pair correlation function, its support and amplitude describe both basis and lattice simultaneously. This is the reason our design principle allows us to design self-assembly of more complicated crystal structures (e.g. the snub hexagonal lattice in Paper III) than what have previously been accomplished.

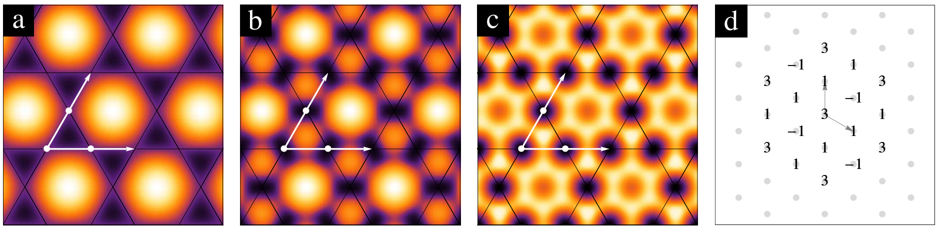

Figure 2.1: *The crystal structure is shown with increased resolution, (**a**)-(**c**), when taking a larger part of reciprocal space (**d**) into account. The numbers signify the structure factors of the reciprocal lattice. The number of reciprocal lattice points for the crystal images are 7,13 and 19 respectively. The white dots and arrows shows the lattice vectors and basis, moving one of the basis coordinates to the vacancy would yield another Kagome lattice. The norms of the structure factors in (**d**) are maximised by the basis for* $|\mathbf{k}| = 2$ *, a negative perturbation of the energy spectrum at this wavelength ensures that the correct basis self-assembles.*

2.3 Examples of designed self-assembled lattices

The constraints outlined above do not completely determine the energy spectrum. Since the energy spectrum can take the form in the region where it's positive, the design principle describes a whole class of interaction potentials that cause self-assembly of the target crystal structure. If the goal is to create an interaction potential that is as simple as possible, one could intend a short range interaction potential which means it falls off quickly in real space, or a smooth one with few complicated features, see Fig. 2.2 for an example. Those two are each others' counterparts after Fourier transforming. A smooth potential is not comprised of Fourier modes with short wavelengths, the high k region of the energy spectrum is zero. Since the energy spectrum and the interaction potential are Fourier transforms of each other the inverse follows: a smooth energy spectrum will translate to a short-range interaction potential. More formally, screening a potential $V(r) \to \xi V(r)$ equates to a convolution in reciprocal space

$$\widehat{\xi V(r)} = \int \mathrm{d}\mathbf{k}\hat{\xi}(|\mathbf{k}-\mathbf{k}|)\hat{V}(k). \tag{2.16}$$

The standard uncertainty relation gives the shape of the most efficient screening function $\xi(r)$ [18] in the form of a limit to how small effect the screening has on the energy spectrum

$$\mathrm{var}[\xi^2]\mathrm{var}[\hat{\xi}^2] \geq \frac{d^2}{16\pi^2}. \tag{2.17}$$

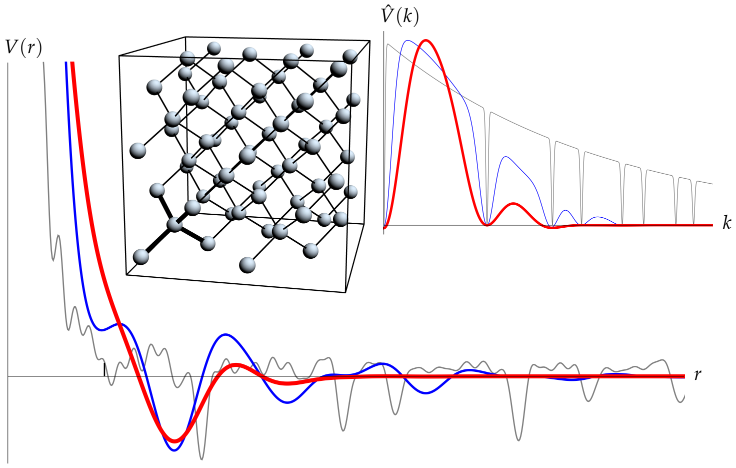

Figure 2.2: *The constraints that guarantees that a target crystal structure (here the diamond structure) is the ground state only requires that the energy spectrum $\hat{V}(k)$ is zero at the support of the reciprocal lattice. Elsewhere, the shape can be chosen arbitrarily as long as it is positive. A naive implementation of these constraints results in very complicated interaction potentials (grey). The interaction potential $V(r)$ can gradually be simplified (blue) using a Gaussian screening and smoothing of the energy spectrum until the point where further simplification would make it impossible to fulfil the constraints (red). The optimally simplified interaction potential (red) still causes a particle system to self-assemble into the target structure, (left inset) shows the diamond structure self-assembled in a Monte Carlo simulation with simulated annealing, simulation and the optimal potential are from Paper IV.*

The screening function that satisfies the lower bound is the Gaussian function, corresponding to a heat kernel smoothing in reciprocal space. This means that for all screening functions with a given level of screening, $\mathrm{var}[\xi^2] = \int \mathrm{d}r \xi(r)^2$ being constant, the Gaussian screening has the smallest impact on the energy spectrum. This means that the interaction potential can be screened more without making it impossible to fulfil the constraints of the design principle. Similarly a heat kernel smoothing of the interaction potential leaves the energy spectrum with a large support than other smoothing operations.

Taking everything we have learned into account, the design principle for targeted self-assembly of crystal structures, as described in Paper IV, is as follows. Create a truncated energy spectrum that covers a bare minimum of the target reciprocal lattice. Add negative-weighted delta functions at k values that coincides with the support of the reciprocal lattice, and perform a small smoothing of the energy spectrum. Gradually increase the smoothing while adjusting the weight and position of the delta functions to maintain the criterion that ensures the target lattice is a ground state. When no more smoothing is possible without breaking the constraints, add small perturbations of the energy spectrum at k values where the norm of the structure factors maxes out by tweaking the corresponding delta functions. Inverse Fourier-transform the energy spectrum in order to obtain a maximally simplified interaction potential that is guaranteed to have the target crystal structure as its ground state.

Another example of the design principle, the obtained interaction potentials and Monte Carlo simulations with the formation of crystal grains and grain boundary diffusion is shown in Fig. 2.3. The simulations was done using local moves and temperature annealing to verify that they do self-assemble into the desired crystal structures under realistic conditions. We assume that the self-assembly occurs at a fixed density that matches that of the target structure and, since any competing configuration will have positive energy, under pressure. Conversely it has been proven that the honeycomb structure cannot self-assemble in free space [19]. This is apparent when looking at the pair correlation function (or the structure factor) versus closely packed lattices with matching and double the unit distance. Since the correlation function for the honeycomb structure can be written as a linear combination of those of the two closely packed structures it cannot be energetically favourable to both.

2.4 Breaking the chiral symmetry

A chiral pattern is defined by its lack of symmetry lines, i.e. its non-superposable with its own mirror image. An example are left and right hands, which are each other's mirror images, they are a pair of enantiomers. Since all distances are preserved in a reflection, it is clear that isotropic interaction potentials cannot be made to differentiate between enantiomers, the energy of the two configurations will be identical. But it was previously not known if an interaction potential could be designed so that the system spontaneously break the chiral symmetry and self-assembles into one of the enantiomers.

The question is interesting from a theoretical point of view. Many types of biomolecules exist only as enantiomers, the chiral form shared among all organisms. The common explanation for homochirality is a spontaneous symmetry-breaking on the microscopic scale leading to a racemic mixture, followed by a chiral specific catalysis or growth that amplifies a stochastic imbalance until the minority enantiomer is gone. Racemic mixtures, chiral auto-catalytic activity and

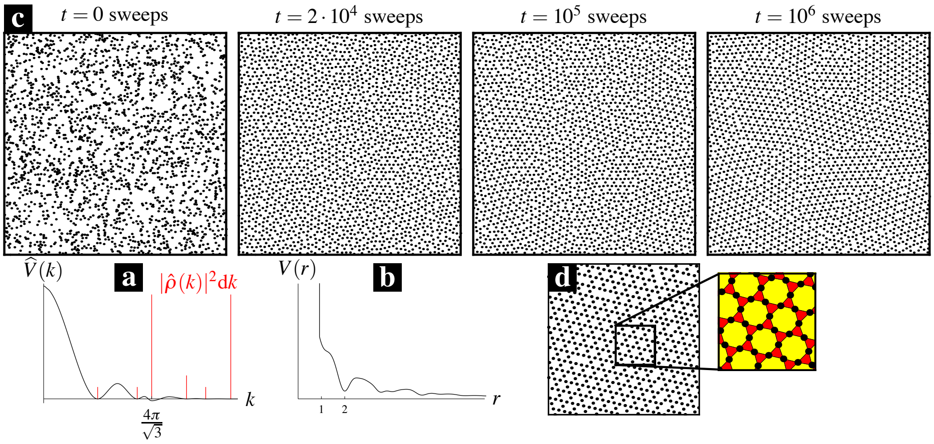

Figure 2.3: *By designing an energy spectrum $\widehat{V}(k)$ (a) with zeroes coinciding with the support of the target reciprocal lattice $\hat{\rho}(k)$ and taking its Fourier transform we arrive at a potential $V(r)$ (b) that causes particles to self-assemble into a target lattice. (c) Time evolution of a self-assembling Kagome lattice in a Monte Carlo simulation. The number of grains diminishes by grain boundary diffusion, a process faster for smaller systems (d) but where some local defects are still present as the dimensions of the system is not fine-tuned to fit the lattice. The example is from paper II.*

the emergence of homochirality have previously been reported in several cases [20, 21], but showing it for a highly symmetric system like the one we model lowered the bar for this to occur. While auto-catalysis is difficult to imagine in a one-component system, crystal growth and diffusion of grain boundaries are still a possible way to obtain homochirality. This changes the question into: is it possible to design a one-component system governed by isotropic interactions that self-assembles into a homochiral crystal?

For a crystal to be achiral there must be some reflection of the structure that would leave both the basis (the most symmetric choice of basis) and lattice unchanged; if there is no such pair of coinciding symmetry lines the crystal is chiral. The simplest chiral structure is a scalene triangle since with all sides of different lengths, a reflection would change the order of occurrence of the side lengths. A Bravais lattice where the smallest occurring triangles are scalene will have no symmetry lines and could be considered the simplest chiral crystal. In reciprocal space, this chirality will manifest in the reciprocal lattice points $\mathbf{G}_i$ which will be arranged in a similar (conserved angles) chiral lattice. We have already concluded in Fig. **??** that any Bravais lattice can be identified and uniquely selected for by a sufficient number of the smallest vertex-vertex distances, even a chiral one which

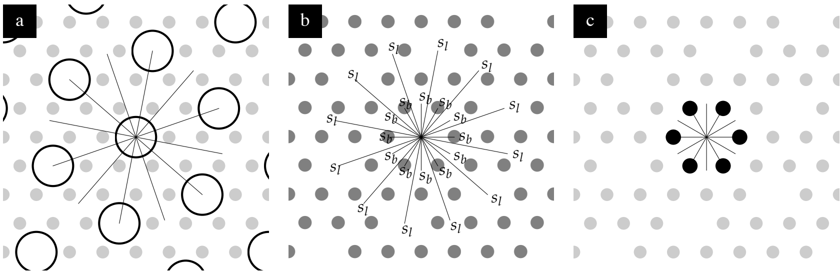

Figure 2.4: *The axes of symmetry of the Bravais lattice (s_l) are highlighted in (a). The Bravais lattice for the snub hexagonal lattice is closely packed. The axes of symmetry of the basis (s_b), which consists of six particles arranged in a hexagonal pattern, are highlighted in (c). Since there are no axes of symmetry that align there is no reflection that keeps the pattern unchanged, therefore the snub hexagonal tiling shown in the figure is chiral.*

we show in Paper III. A less obvious type of chiral lattice is one where the symmetry axis of the basis and those of the lattice are unaligned, Fig. 2.4. Now the chirality must instead manifest in the structure factors in reciprocal space. One such example is the snub hexagonal tiling, a triangular lattice with a basis of 6 particles, arranged in the shape of a hexagon (both with 12 symmetry lines), this is also possible using the design principle outlined in this chapter, Fig. 2.5, which we showed in Paper III.

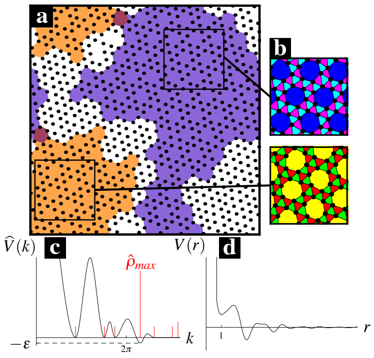

Figure 2.5: *(a) Grains of snub hexagonal lattices, self-assembled from a Monte Carlo simulation. (b) The emerging chirality can be either left- or right-oriented. (c) By selecting for the reciprocal lattice (the red peaks) of the target structure, with a negative perturbation ε where $\hat{\rho}$ is maximised, we obtain a potential (d) which causes self-assembly into the target structure. The example is taken from Paper III.*

Chapter 3

Fourier modes as universal patterns

There are many theoretical results one can pursue on the topic of targeted self-assembly. A design path for calculating or deducing interactions that cause self-assembly of different structures, like DNA origami [13] or the principle presented in the last chapter, are examples of this type of results. Another is understanding and identifying universal patterns, wide classes of interactions that cause self-assembly into only a few types of patterns. From a design perspective, a theoretical explanation for a set of universal patterns tells us what kind of structures one can expect being easy to self-assemble and how to achieve that in the most efficient way possible.

Calculating the ground state for a system with an arbitrary set of interactions is an unsolved problem, but as we show in Paper I, V and VI an approximate model can yield insight into what features the ground state configuration is defined by. Here, this approximation takes the form of relaxed constraints on the density function in reciprocal space $\hat{\rho}(\mathbf{k})$. This makes it possible to predict and design the self-assembling patterns of particles interacting with long-range isotropic interactions.

3.1 The spherical model

If we are only interested in the formation of patterns on a scale significantly larger than that of individual particles (as opposed to when trying to differentiate between, for example, hexagonal closely-packed and cubic packing), using a finite resolution model resolved on a lattice does not detract from our ability to describe the system. For a lattice system, where each of N sites at coordinate

$\mathbf{r}_i$ takes the value $u_i \in \{0,1\}$ depending on whether a particle resides there, the configuration energy becomes

$$E = \sum_{ij} u_i u_j V(|\mathbf{r_i} - \mathbf{r_j}|) = \mathbf{u}^\top J \mathbf{u} \tag{3.1}$$

where $V(r)$ is the interaction function, and the interaction matrix with elements $J_{ij} = V(|\mathbf{r_i} - \mathbf{r_j}|)$ describes how particles at different lattice sites interact with each other. This description of the particle configuration comes with constraints, namely that the sites can only take values 0 and 1, and that they sum up to n, the total amount of particles. These constraints can also be formulated in terms of moments of the lattice vector $\mathbf{u}$

$$\sum_i u_i^m = n \; \forall m \in \mathbb{N}. \tag{3.2}$$

While the energy expression is quadratic, we still cannot solve the problem due to the constraints on the higher order moments. If we relax the constraints to only include the first two moments, $m \leq 2$, the problem becomes quadratic and exactly solvable. This is the spherical model, Paper I. The model is akin to a low-resolution picture of the exact system, with "soft" particles as the density limit is only given by the total number of particles and not by any limit on packing efficiency. The low-resolution equivalence that one obtains from this approximation exhibits in many cases striking similarities with the behaviour of particle systems.

Edlund and Nilsson Jacobi lay the foundation for how the spherical model can be used to address self-assembly by noticing that matrices from isotropic interactions commute [11], and thus share a common eigenbase that diagonalises the energy expression $J\mathbf{v_k} = \lambda_\mathbf{k}\mathbf{v_k}$. In two dimensions with periodic boundaries, the base is Fourier modes. Just like in the continuum case, this turns the problem into a tractable one when expanding the configuration in terms of the eigenvectors $\mathbf{u} = \sum_\mathbf{k} c_\mathbf{k}\mathbf{v_k}$

$$E = (\sum_\mathbf{k} c_\mathbf{k}\mathbf{v_k}^\top) J (\sum_\mathbf{k} c_\mathbf{k}\mathbf{v_k}) = \sum_\mathbf{k} \lambda_k c_\mathbf{k}^2 \tag{3.3}$$

since the eigenvectors are orthogonal. λ_k is the discrete counterpart to the energy spectrum in the previous chapter and just like in the continuous case it is degenerate for a fixed norm of $\mathbf{k}$. The constraints on the first and second moment also translate well to the eigenbase

$$c_{\mathbf{0}} = \frac{n}{N} \tag{3.4}$$

$$\sum_{\mathbf{k}\neq\mathbf{0}} c_{\mathbf{k}}^2 = \frac{n(N-n)}{N^2}. \tag{3.5}$$

Combining Eq. 3.3 and Eq. 3.5 shows that the ground state configuration of the spherical model is one where all weight is put on Fourier modes with the lowest eigenvalue (with the exception of $c_{\mathbf{0}} = n/N$). For almost any long-range interaction potential, the space filling ground state turns out to be striped (or spotty if the particle density is low), a pattern defined by a single wave length. From a design perspective the energy spectrum makes it easy to create an interaction potential that causes a striped pattern with a specific wavelength to self-assemble [11].

The interaction matrix J_{ij} can be written as a linear combination of discrete Laplace operators, $J = \sum \alpha_{lm} \Delta_+^l \Delta_\times^m$ with Δ_+ defined as the discrete Laplace operator on a lattice and $\Delta_\times$ being the diagonal equivalence. The contribution to J from $\Delta_+^l \Delta_\times^m$ will have a maximum interaction length given by $\sqrt{(l+m)^2+m^2}$ lattice distances; by adjusting α_{lm} for all distances on the lattice, starting with the longest, any isotropic potential can be represented. Fourier modes are eigenvectors to the Laplace operator and therefore also to $\Delta_+^l \Delta_\times^m$ and J. While we knew before that Fourier modes diagonalises the interaction matrix, this representation does point to a subtlety; the eigenfunctions f of the Laplace operator $\Delta f = \lambda f$ depend on the boundary conditions of the system. By requiring that the system should converge towards zero at infinity, the translational invariant Fourier modes no longer fit the bill, but radial Bessel functions around any finite point with an angular modulation $f = J_\omega(2\pi k r)\cos(\omega\theta)$, both converge at infinity and are eigenfunctions to the Laplace operator. The generalisation to three dimensions is straightforward, resulting in spherical harmonics. The eigenvalues are independent of which eigenbase we use.

Since eigenvalues for fixed k value are degenerate, the energy of the spherical model is minimised once again by a combination of spherical harmonics corresponding to the minimum of the energy spectrum. In order for the constraint on the first moment to be fulfilled, a mass building term has to be added as well

$$\sum_{\omega=0}^{\infty} c_{\omega,\kappa} J_\omega(2\pi\kappa r)\cos(\omega\theta) + c_m J_0(2\pi k_m) \tag{3.6}$$

in the limit $k_m \to 0$. Just like there are many linear combinations of Fourier modes that do not look like stripe patterns, the set of solutions to the spherical model using spherical Bessel functions is too broad. The question is which combinations are closest to a binary solution. If we do find a solution that is very close to binary, we can expect it to be a universal pattern since as long as we can rescale the pattern so that it matches the global minimum of an energy spectrum $\lambda_{k_{min}}$, the energy will be close to the theoretical lower limit

$$\sum_{\mathbf{k}} \lambda_k c_{\mathbf{k}}^2 \geq \frac{n(N-n)}{N^2} \lambda_{k_{min}}. \tag{3.7}$$

When expanding a square wave into Fourier modes, overtones are what differentiate the base frequency Fourier mode from its square wave counterpart, see Fig. **??**. Just as for the square waves, overtones in the Bessel base are multiples of the base frequency, and it turns out that just a few terms of the sum suffice to recreate most commonly occurring patterns assembled from random interactions, Fig. 2 in Paper I.

$$\sum_{n=\{1,2,3...\}} a_n J_{n\omega}(2\pi k_{min} r) \cos(n\omega\theta) + c J_0(2\pi k_m). \tag{3.8}$$

In Paper I We created an ensemble of solutions on this form of the spherical model with Dirichlet boundary conditions on a small disk, with k_m and k_{min} values chosen so that the eigenvectors satisfied the boundary conditions and mapped them to binary-valued patterns using a threshold for mapping to 1 to control n. These were candidates for universal patterns. We generated random continuous piecewise linear interaction potentials until we had $1,000$ that caused an aggregating pattern, i.e. where the global minimum was at $k = 0$, and scaled the interaction range so that the non-origin minimum in the energy spectrum coincided with $k_{min} = 1$. A few generated patterns stand out as energetically favourable for a large amount of interaction potentials, Fig. 3.1.

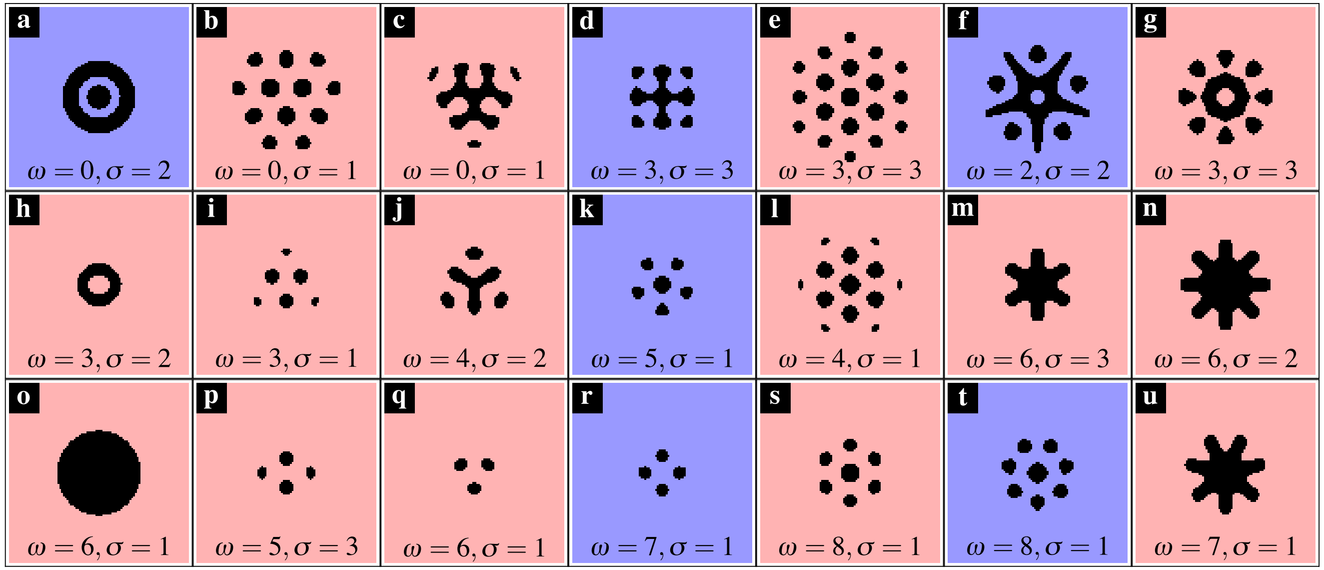

Figure 3.1: *The predicted morphological alphabet for aggregated particle structures, generated from Bessel functions with base angular frequency* $\omega \leq 8$ *and the cut-off limiting the nuclei size to up to three radial oscillations* ($\sigma \leq 3$)*. Colour indicates the signal strength of the prediction, i.e. how large a fraction of the randomised potentials were found to prefer it. Red background signifies a strong signal, blue weaker.*

To summarise the theory predicts that all of these patterns will be low-energy states for most interaction potentials that cause large-scale aggregate patterns. The patterns are almost exclusively defined by the characteristic length scale and their energy therefore close to the theoretical minimum for the spherical model with relaxed constraints, compared to a binary-valued lattice. Which of the patterns that assembles for a given interaction potential will depend on the number of particles in combination with how well secondary features of the energy spectrum match the different patches. To test this prediction, we ran simulations of self-assembling particle systems for random interaction potentials (piecewise linear like before but also generated as third order splines) and looked at how well typical patterns matched our alphabet. Out of 1200 interaction potentials that caused aggregation (a global minimum in the energy spectrum at $k = 0$), approximately 86% are described by the limited alphabet and 9% of the remaining self-assembled patterns are described by Eq. 3.8 but require more terms to be represented accurately than we tested for in our parameter sweep. Typical patterns that self-assembled in the simulations are shown in Fig. 3.2.

3.2 Generalising to multiple particle types

As a universal pattern, stripes are a commonly occurring phenomenon. One example, interesting due to its possible applications in self-assembly, that has been reported to self-assemble into the type of striped patterns the spherical model describes so well is that of alkanethiol-coated gold nanoparticles [22]. While the reliability of the experimental results is debated, detailed simulations of the same system show that alkanethiol molecules of several different lengths segregate into patterns of stripes and spots [23]. The stripes and spots are the result of a conflict between immiscibility of different types of alkanethiols and an entropic mixing in order to increase the free volume for longer molecules. In Paper V we predict which combination of stripes and spots would form from the interactions among the surface constituents. While the binary lattice model discussed previously could represent two particle types that together are space-filling just as well as it represents one type in a vacuum, in order to describe three or more types we need to generalise the model.

The complete orientation of the surface molecules requires too many degrees of freedom to capture with a lattice model. Since our interest is the relation between energy and surface pattern, we restrict ourselves to a lattice model describing where different alkanethiol molecules stick to the nanoparticle surface. This means that the interaction potential describes the effective interaction (in-

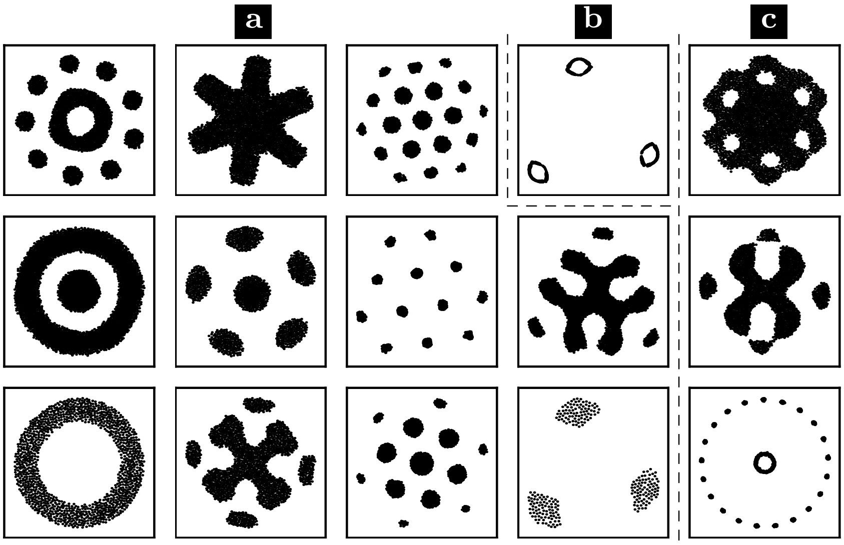

Figure 3.2: *Examples of low energy states from Monte Carlo simulations of large particle systems with randomised interactions. (a) Most interactions cause patterns predicted by the morphological alphabet. Some exceptions (b) are hierarchical structures where each part of a predicted pattern work as a nucleation point for another morphological structure. (c) some patterns were not predicted in Fig. 3.1, despite that they can be described by Eq. 3.8.*

cluding terms with entropic origin) between molecules attached to the surface, as a function of the distance between their anchor points. The spherical model is expanded to encompass a lattice for each type t of alkanethiol molecules (with a finite number T of distinct types). Then the vector $\mathbf{u}$ consists of T segments of length N, $\mathbf{u}_t$, each describing the amount of particles of type t on the different lattice sites with 1 indicating that the site is occupied by a particle of type t. The total energy of the system can still be written using matrix multiplication

$$E = \sum_{s,t=1}^{T} \mathbf{u}_t^\top J_{ts} \mathbf{u}_s = \mathbf{u}^\top J \mathbf{u}. \tag{3.9}$$

Each of the $T \times T$ blocks in J is an isotropic matrix representing how a pair of surface types interact, Fig. 3.3. These are diagonalised blockwise by the solutions to the Laplace equation on a spherical surface; spherical harmonics Y_l^m (l and m are orbital numbers). The sub matrices' eigenvalues form a $T \times T$ matrix Λ_l that describes how a superposition of spherical harmonics of the different surface types is related to the energy. Due to rotational invariance, the eigenvalues are

$$\begin{pmatrix} J^{11}_{11} & \cdots & J^{11}_{1\mathrm{N}} & \cdots & \cdots & J^{1\mathrm{T}}_{11} & \cdots & J^{1\mathrm{T}}_{1\mathrm{N}} \\ \vdots & & \vdots & & & \vdots & & \vdots \\ J^{11}_{\mathrm{N}1} & \cdots & J^{11}_{\mathrm{NN}} & \cdots & \cdots & J^{1\mathrm{T}}_{\mathrm{N}1} & \cdots & J^{1\mathrm{T}}_{\mathrm{NN}} \\ \vdots & & \vdots & & & \vdots & & \vdots \\ \vdots & & \vdots & & & \vdots & & \vdots \\ J^{\mathrm{T}1}_{11} & \cdots & J^{\mathrm{T}1}_{1\mathrm{N}} & \cdots & \cdots & J^{\mathrm{TT}}_{11} & \cdots & J^{\mathrm{TT}}_{1\mathrm{N}} \\ \vdots & & \vdots & & & \vdots & & \vdots \\ J^{\mathrm{T}1}_{\mathrm{N}1} & \cdots & J^{\mathrm{T}1}_{\mathrm{NN}} & \cdots & \cdots & J^{\mathrm{TT}}_{\mathrm{N}1} & \cdots & J^{\mathrm{TT}}_{\mathrm{NN}} \end{pmatrix} \Rightarrow \begin{array}{c} \begin{pmatrix} \Lambda_{11} & \cdots & \Lambda_{1K} \\ \vdots & & \vdots \\ \Lambda_{K1} & \cdots & \Lambda_{KK} \end{pmatrix} \\ \vdots \\ \begin{pmatrix} \Lambda^{l}_{11} & \cdots & \Lambda^{l}_{1K} \\ \vdots & & \vdots \\ \Lambda^{l}_{K1} & \cdots & \Lambda^{l}_{KK} \end{pmatrix} \\ \vdots \end{array}$$

Figure 3.3: *Each part of the interaction matrix describing the interaction between two particle types are diagonized by spherical harmonic functions. This allows the Hamiltonian to be written as a sum over l-degrees (energies associated with equal degrees l but different orders m are degenerate) and the matrices' sizes to be limited by the number of particle types T rather than the spin model resolution.*

degenerate with respect to m. The orbital number l defines the length scale of the harmonics, and as in the two dimensional case, we are primarily interested in the length scale at which different types will separate.

We can diagonalise Λ_l individually for each l value. The T eigenvalues to these matrices form our new energy spectrum. The corresponding eigenvalues represent which types segregate from the others, e.g. the eigenvalue -1 with the corresponding eigenvector $\{1,1,-1,0\}$ of Λ_l signifies that the first and second type segregating from a third type (elements with different sign in the eigenvector) at length scale l is associated with energy -1. For every length scale there will be T eigenvalues, each representing the energy associated with a segregation between different constellations of the types. The solution to the spherical model will simply be one consisting of Y_l^m terms where l matches the global minimum of the energy spectrum (plus a global offset from Y_0^0).

The energy spectrum with its multiple branches becomes a powerful tool for predicting which pattern has the lowest energy, and ultimately for designing that pattern, when the stoichiometry is fixed. Since we only have to consider patterns consisting of stripes and spots of wavelengths corresponding to minima in the energy spectrum. The role of the fixed stoichiometry is to, combined with the energy spectrum determine which combination of stripes or spots takes precedence. The global minimum of the energy spectrum still dominates which pattern forms, but only up to how much the stoichiometry allows. After that at which length scale the remaining types segregate will be determined by the second (applicable) minimum of the energy spectrum, and so on. Whether a segregation causes

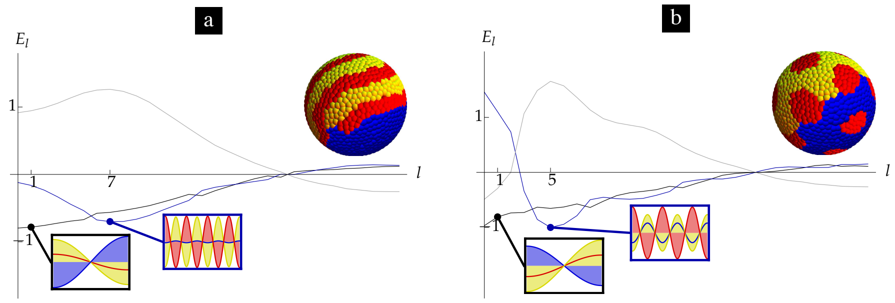

Figure 3.4: *Energy spectra calculated from piecewise constant interaction potentials with a shallow long range attractive basin and a short range shoulder potential. (a) The global minimum at* $l = 1$ *causes blue to segregate from the other two types since they have different sign in the eigenvector (inset at* 1*). The red and yellow region in turn form a striped pattern with a length scale defined by* $l = 7$ *(inset at* 7*). (b) If the order of the minima is reversed, the red segregates from the blue and yellow at a length scale defined by* $l = 5$*. Since there is less red than blue and yellow combined, the red type forms spots. The minimum describing how blue and yellow segregats show that they form a Janus pattern outside the red spots. The surface patterns were self-assembled by Monte Carlo simulations with simulated annealing. The examples and energy spectra were taken from Paper V.*

stripes or spots depends on if the segregating quantities are balanced. Fig. 3.4 illustrates an example of a self-assembling surface pattern of three types, red, yellow and blue, each of equal amount on the surface. If the global minimum of the energy spectrum is at $l = 1$ ($l = 0$ eigenvalues describe how the stoichiometry influences the energy), with the corresponding eigenvector $\frac{1}{3}\{1,2,-1\}$ signifying that the red and yellow will phase-separate from blue, creating a large patch on one side of the sphere. At the second minimum at $l = 7$, the corresponding eigenvector has different signs for red and yellow; $\frac{1}{\sqrt{14}}\{3,-2,-1\}$ and thus determines the length scale of the striped pattern on the red-yellow part of the sphere. If the order of the minima is reversed the ground state pattern is instead one with red spots on a yellow-blue Janus sphere[1]. Red creates a spotty pattern against a yellow-blue background as there are many fewer red than blue or yellow types. The second minimum at $l = 1$ segregates the yellow-blue regions into a Janus-like pattern.

---

[1] Technically, the defining property of a Janus sphere is that it's surface has regions with different physical properties. It is commonly used, so also here, to signify a particle with two distinct parts, half of the particle has one type of surface and the other half another type.

Chapter 4

Hierarchical self-assembly

Universal patterns can also be utilised in targeted self-assembly. This is often beneficial since the universal patterns are robust and not sensitive to details of the interactions. But this also indicates that designing self-assembly of a pattern not among the universal ones is more difficult. A system that self-assembles into the same pattern even when system parameters change significantly will inevitably have fewer regions with distinct behaviours. A possible way to expand the repertoire that simultaneously depends on reliability is hierarchical self-assembly: a system that self-assembles into building blocks that in turn arranges themselves into more complex structures. The two most recent articles of this thesis concern systems in which the possibility of hierarchies of self-assembly is of central interest.

4.1 Patchy nanoparticles

Anisotropic colloids show great promise for self-assembly of complicated structures. More and more fabrication techniques are developed, and these can now take the shape of for example cubes, rods and ovoids, and even surface carvings moulded from other nanoparticles [24]. Similarly, glancing angle deposition and other techniques are used to create patterns of attractive or repulsive patches on the surface of nanoparticles, allowing us to control how the building blocks are allowed to connect to each other [25]. However, there are limitations to any fabrication technique, and the type of universal striped and spotty patterns discussed in the previous chapter are quite different from what previous methods are capable of. The idea of using the spontaneous forming of surface patterns on coated

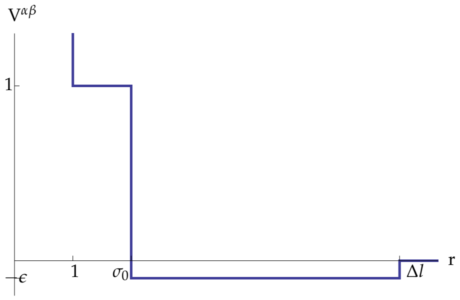

Figure 4.1: *The model's interaction functions between different particle types consists of a shoulder potential reaching neighbouring particles, an attractive basin indirectly set by the relative length of the alkanethiol molecules and a hard core. By using the design principle presented in Paper VI we find values for the depth of the attractive basin, ε, and the reach of the alkanethiol molecules, that causes different functional patterns to self-assemble..*

nanoparticles to obtain patchy colloids, which in turn self-assemble into other structures is therefore exciting.

The mathematical foundation for how to design hierarchical self-assembly of coated nanoparticles in Paper VI is not tied to a specific set of interactions, type of surface or coating, but rather follows a few general criteria. The individual molecules or polymers that coat the nanoparticle surface must be able to rearrange, and behave as if interacting with each other according to an effective middle-range interaction potential. In a broader sense, the universality of striped and spotted patterns indicate that when a striped pattern have been observed to self-assemble, much more interesting surface patterns are also obtainable as long as one can influence which length scale the striped pattern will prefer and with a good control of the stoichiometry. The competition between short range immiscibility and middle range mixing of two different types of alkanethiol molecules on gold nanoparticles can be captured by a simple piecewise constant function, with an attractive basin at middle range and a shoulder potential at short range for surface constituents, Fig. 4.1. This model leaves us with the same degree of control over how the coating interacts, and allows the same type of surface patterns to self-assemble as first principle simulations of this type of system [23]. While it can't provide us with actual experimental parameters to test, it serves as an illustration of how this level of control over the surface coating allows functional patterns to self-assemble into building blocks, which in turn self-assemble into geometric structures.

The gist of the spherical model for multiple surface types in Paper V is that we can calculate an energy spectrum directly from the effective interaction potential of our model system. The global minimum of the energy spectrum predicts the length scale at which certain surface types will segregate from each other. With a fixed stoichiometry the other minima of the energy spectrum will describe how the remaining types segregate in the order of lowest energy to highest. The fact that the ground state can be related to the energy spectrum makes it much easier to design a system that self-assembles into a target system as well. The universality of patterns consisting of spots and stripes means our target pattern should be of that form as well.

Say that we want to self-assemble a crystal structure, like the cubic lattice or a diamond structure. The simplest surface pattern that causes self-assembly into those structures would be 4 resp. 6 attractive patches evenly distributed on the surface of the sphere. Expanding the target patterns in terms of spherical harmonics show that they are defined by length scales $l = 3$ and $l = 4$. By tuning the parameters of the model, in this case the strength of the entropic mixing and the relative length of the alkanethiol molecules, we find parameters settings where the energy spectrum of the simplified model exhibits minima at $l = 3$ and $l = 4$. A sufficiently imbalanced stoichiometry will cause the ground state to be a spotty pattern, which is confirmed in Monte Carlo simulations to form the desired functional surface pattern of 4 or 6 patches. Subsequent Monte Carlo simulations of patchy particles with the assembled surface pattern, where the spots are attractive, show that they self-assemble into the intended crystal structures, Fig. 4.2.

For more complicated functional surface patterns, more elaborate energy spectra have to be designed. To self-assemble small cubic aggregates the most efficient surface pattern is three orthogonal red patches against a blue background, defined by the $l = 4$ length scale. A minimum at $l = 4$ is the first necessary feature in the energy spectrum. We also need a way to localise the three patches to one side of the nanoparticle. This means a third surface type, yellow, that prefers to segregate from the components of our patchy pattern at low l values, i.e. promoting the formation of a Janus sphere. In order to make the patches small so that the nanoparticles must align more perfectly for the patches to stick to each other, a third feature at around $l = 8$ in the energy spectrum is added that separates blue and red regions from each other by the third yellow type, resulting in smaller red and blue regions (if the stoichiometry is changed to match the energy spectrum), this is illustrated and verified by simulations in Fig. 4.3. An interesting detail is that the red-blue patchy region of the Janus sphere is an aggregate pattern, predicted by the alphabet of universal aggregate patterns in Paper I, Fig. 3.1 j.

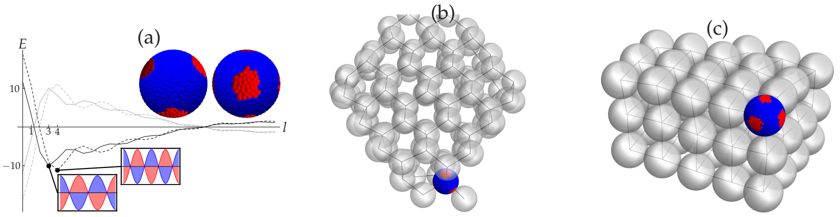

Figure 4.2: *(a) A phase separation at* $l = 3$ *together with a 4:1 ratio of blue:red surface constituents causes the ground state configuration to have four equally separated patches (solid line, left inset in a). With the minimum at* $l = 4$ *and a blue:red ratio of 3:1, the types self-assembles into 6 patches instead (dashed line, right inset in a). On the colloidal scale, the small changes make the difference between a self-assembling diamond lattice (b) or a cubic lattice (c). Both surface patterns and the colloidal structures are obtained from Monte Carlo simulations using simulated annealing. The parameters in the model, Fig. 4.1, the details of the Monte Carlo simulations can be found in Paper VI.*

4.2 Self-assembly in biology

One of the main issues with technological advances using designed self-assembly is that when a large part of the material composition is designed to cause a desired pattern to self-assemble, there is less opportunity to obtain desired material properties. And many types of materials rely on a scale too small to allow for much design at all; the mechanical properties of diamonds stem from the atomic structure, and the resolution on experimental silica circuits are quickly getting close to the limit set by atomic scale [26]. One type of systems with already built-in and tuneable mechanisms for complicated interactions governing self-assembly are biological systems. How cells divide, rearrange and form structure is a type of self-assembly on many levels, from protein and DNA-folding to cellular morphogenesis, and with sufficient understanding of these processes we can influence and design the outcome by making changes in the genetic code. There are also a wide range of existing traits and properties in nature that we already imitate (biomimetics) or transfer over species barriers (genetic engineering) like chemical factories [27] in cells, the stickiness of gecko feet [28], the super (water) repellent surface of lotus leaves [29] or even growing replacement organs and tissues in medical science [30].

In line with our work on self-assembling particles into structures, my latest work on self-assembly concerns the possibility of designing self-assembling structures by encoding for simple growth rules in cells. While cellular morphogenesis is governed by many mechanisms like cell motility, cell specialisation

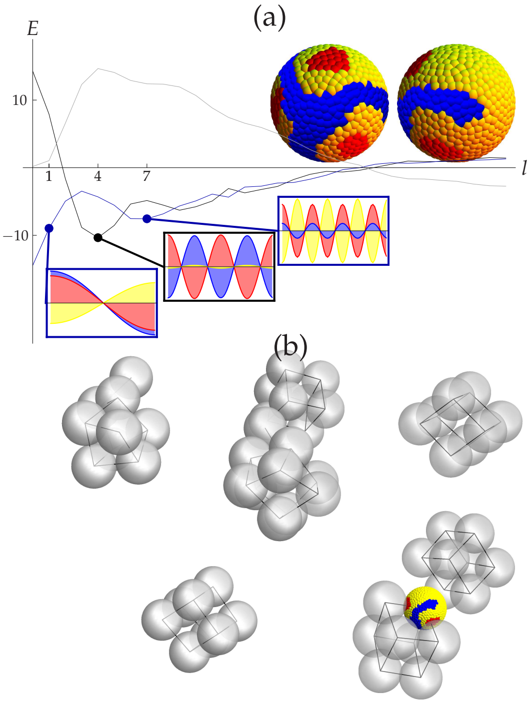

Figure 4.3: *With greater control over the energy spectrum, more complex functional patterns can be made to self-assemble. (a) Here three minima in the energy spectrum together encode for a pattern of three orthogonal red patches with high specificity. The first minimum concentrates red and blue to one side. The second minimum causes red patches to be separated by blue regions with a desired distance. The last minimum causes red and blue regions to be separated by yellow, allowing for a higher specificity. b) Hierarchical self-assembly of cubic aggregates when the red patches are attractive. Both the surface pattern and the patchy particle configuration were obtained by Monte Carlo simulations with temperature annealing. Interestingly, the red-blue pattern is an aggregate pattern, and was predicted by Paper I, see Fig. 3.1 j. The energy spectrum and the simulations are taken from Paper VI, more details can be found in the paper.*

etc., my goal is not primarily to recreate how existing organisms and cell colonies grow but rather to build a framework for controlling growth patterns using as few mechanisms as possible. Contrary to particle self-assembly, cellular morphogenesis does not find the molecular ground state configuration. While the system on all hierarchies change along the energy gradient the many hierarchies of reactions in a cell makes it much more natural to describe the growth in terms of cell behaviour, i.e. in what situations cells grow and how cell growth and cell division alter the cell structure.

The draft paper in the Appendix uses a spring network model to describe how cells move around and change shape under the influence of external forces, a kind of model that previously has been used to explain local cell structures [31], see Fig. 1 in the draft paper in the Appendix. The mechanism behind cell division is described by internal timers counting down towards the next cell division at a rate determined by the types of the surrounding cells. The article focuses on what kind of growth patterns of one or two different cell types the growth mechanism can sustain. The growth rules are encoded for with a series of scalar values and could for example signify that green cells grow in the vicinity of red cells but never on their own, or that red cells grow quicker the more red cells to which they are adjacent to. The model is, despite its simplicity, rooted in reality.

It turns out that the growth rules make a wide range of patterns accessible, Fig. 4.4 (right). Of special interest is the formation of protrusions, shells and strongly mixed regions of the two cell types as they could be considered building blocks for more complicated patterns and are the most basic forms of functionality: reach, protection and surface area. By analysing random growth rules that cause the cell cluster to form any of the three interesting patterns and comparing them to what surroundings the different cells experience, it is possible to understand the mechanism behind these growth patterns. For example, the most efficient way to cause cells of one type to form a protective shell around another cell type turns out to be a set of growth rules where the interior cells grow when exposed to the protective shell. The shell in turn grows as a consequence of the cells in the shell being stretched thin by the growing interior, Fig. 4.4 (right). For the growth of thin protrusions, the rules should instead promote growth only for cells that are exposed the most to the outside, i.e. on the tip of the protrusion, in combination with a high cell adhesion in order to keep the growing protrusion centred. As of now, the model has no built in mechanism for ending or changing the growth once a certain size is reached or time has elapsed. But once the growth rules have been tied to a gene regulatory network (or another mechanism rooted in biology) we should be able to design hierarchical self-assembly in the

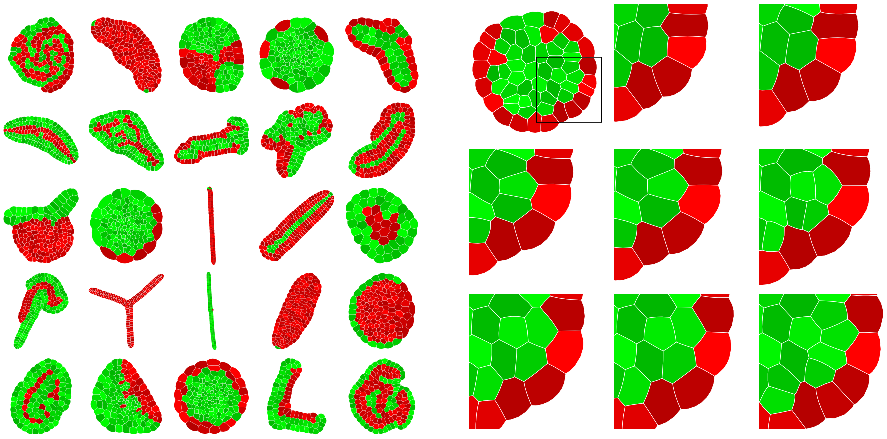

Figure 4.4: *(left) Examples of growth patterns caused by randomly generated growth rules. Among these are shells of various thickness, growth along the surface of other cell types and alternative mechanisms for protrusion growth; using a single green cell as catalyst for growth or protrusions with a shell. (right) A time series of a cell growth simulation that forms a shell. Green cells exposed to the interior of the shell divide, when the shell is stretched thin, the red cells divide. The examples are from the draft paper in the Appendix.*

cell model as well.

Chapter 5

Overview of scientific results

The theme of this dissertation is designing and predicting self-assembling systems without resorting to trial and error schemes, which would become more and more time-consuming as the complexity of the system increases. The articles describe different approaches or tools to circumvent or reduce the need to test a self-assembling process in order to evaluate the feasibility of the assembly process. All but the last of the articles are based on representing a self-assembling system in terms of Fourier modes in order to analytically calculate features related to a ground state.

Draft paper: Shape self-regulation of basic cell patterns interacting via cell adhesion

The draft paper in the Appendix is one step removed from the previous articles that consider models with interactions reasonable in colloidal systems. Considering that life is a form of self-assembly, this article explores the possibilities of designing cell growth patterns assuming one could influence and tune the requirements for cell division. The article focuses on two fundamental patterns, protrusions and shells, and explains the most efficient mechanism behind the growth of these patterns. The most interesting is the mechanism behind shell growth, where cells divide along the interior of the surface shell causing it to stretch. The stretching of the surface layer triggers cell division leading to a one cell layer thick shell that adjusts its growth rate to the cells inside the shell.

Paper I: Novel Self-Assembled Morphologies from Isotropic Interactions

In Paper I we expand the theory explaining universality of stripes to consider small systems where space-filling morphologies are excluded due to the limited number of particles available. This is used to obtain a series of morphologies that can be considered universal for large-scale nucleating (two-dimensional) systems with isotropic interactions. The morphologies are discrete approximations to spherical Bessel functions with angular modulation, a set of functions that solve Laplace's equation just like Fourier modes, with the difference being that the Bessel functions are localised. An investigation of randomised interactions supports the claim of a predicted alphabet of universal patterns. A universal alphabet of available patterns can be expected to be valid for other models or systems than the one used for validation, as well as tell us something important about limitations to self-assembly in whole class's of systems.

Paper II: Designing Isotropic Interactions for Self-Assembly of Complex Lattices

Paper II uses Fourier analysis to obtain a direct method for finding isotropic interactions that cause self-assembly into target crystal structures. The reciprocal representation of a crystal structure will only consist of Fourier modes with wavelengths that coincide with the periodicity of the lattice. By creating an interaction function that has higher energy for configuration with any other periodicity present, one can guarantee that the target lattice is the ground state. As long as the lattice basis is not too complicated, small perturbations of the interaction function allow the target crystal to become the ground state. The method is applied to a series of crystal structures as examples chosen for their varying complexity and occurrence in recent publications.

Paper III: Chiral Surfaces Self-Assembling in One-Component Systems with Isotropic Interactions

In the third paper, Paper III, we prove that the mirror symmetry can be broken without relying on anisotropy of the constituent particles, further pushing the boundaries for what is considered achievable with isotropic interactions. There are two types of chiral crystals, either the Bravais lattice that defines the periodicity is chiral in itself, or the base of the lattice is the cause of chirality. The article brings up an example from both categories as well as investigates the effects of perturbations from the derived interaction potential.

Paper IV: Using the uncertainty principle to design simple interactions for targeted self-assembly

Paper IV provides theoretical arguments for how to make the derived class of interaction potentials from the previous two articles as short-range and smooth as possible, while still ensuring that the target lattice is a ground state. Optical properties of a material are closely tied to its reciprocal representation and by penalising certain length scales in a model solution, it is possible to create an optical band gap in the solution. The width and quality of the optical band gap is also related to the complexity of the interaction function that caused it.

Paper V: Predicting self-assembled patterns on spheres with multicomponent coatings

Paper V is a generalisation of the theory underlying Paper I and [11], to include multiple particle types. The paper describes a principle for deducing the combination of stripes and spots assembled on the surface of spheres when the stoichiometry is fixed. The principles are general, but the model used for validation and confirmation is a minimalistic representation of alkanethiol molecules adsorbed to gold nanoparticles. Diagonalisation of the Hamiltonian provides an energy spectrum stating at which length scale the different surface constituents prefer to segregate. The ground state is a combination of stripes and spots from these segregations, where the most energetically preferred segregation dominates and constrains the subsequent segregating constituent types.

Paper VI: A design path for hierarchical self-assembly of patchy colloids

Paper VI combines the principles of all the previous articles in order to design hierarchical self-assembly. The interaction between different surface constituents on spherical particles is designed so that they self-assemble into functional patterns, with patches oriented in directions that allow for self-assembly of the spherical particles themselves into geometrical structures. An example could be a surface coating of three types on nanoparticles, one segregating from the others forming a Janus sphere, the other two segregating on a shorter length scale causing an aggregate pattern from among those published in Paper I, a pattern including three patches now separated at right angles from each other. If those patches can be made attractive, they cause self-assembly of cubical aggregates of the nanoparticles.

Chapter 6

Summary and outlook

This thesis outlines a theoretical framework for addressing problems of self-assembly of particle systems with isotropic interactions. It is based on expressing the energy of particle configurations in terms of an orthogonal base, which due to the symmetry of the interactions are independent of the interaction potential. Prediction and design becomes easier in this basis because the energy contributions from different wavelengths are independent. The interaction potential instead determines the energy associated to different wavelengths, creating an energy spectrum of which the minimum almost completely defines what kind of pattern the interactions will cause. Paper I expands on a previous article [11] that explains the universality of striped patterns. The eigenfunctions changes for different boundary conditions and similarly to how planar waves describes the space filling and universal striped pattern, switching to polar coordinates with Dirichlet boundary conditions give a base much more suitable to describe particle patterns that aggregate around a nucleation point: spherical Bessel functions with angular oscillations. With this new perspective we predicted a set of universal aggregate patterns that was in good agreement with simulated self-assembly from randomised interactions. The universality of these patterns means that they are expected to be obtainable patterns in vastly different systems, but it also means that patterns not found among those of the predicated alphabet are very unlikely to self-assemble.

The eigenbase consists of Fourier modes when the boundary conditions are periodic, also, they also ideal for describing crystal structures. A natural goal for targeted self-assembly is to be able to design interaction potentials causing crystal structures to self-assemble. Paper II presents a design scheme that guarantees that an interaction potential satisfying a series of constraints will have a target crystal structure as its ground state. Paper III and Paper IV gradually expands on what can be made to self-assemble using the design scheme, and how to use the nature of the necessary constraints to minimise the complexity of the derived interaction potentials. The design principle was verified for different crystal structures, the Kagome lattice, the diamond structure and chiral crystals for example.

The last part of the thesis discusses Hierarchical self-assembly. If there exist universal patterns that easily self-assembles for many different interactions, it means that it is less likely for other structures to be obtainable. One way to expand the repertoire of structures that can reliably form is to consider self-assembly of structures or building blocks that in turn self-assembles into a target structure. A real world system where this might be feasible is alkanethiol-coated gold nanoparticles. By designing the stripe- and spot-pattern that is formed by different surface molecules, it is possible to make the nanoparticles have patches in many different directions and of many different shapes. Paper V and Paper VI are a generalisation of the earlier work to multiple particle (representing alkanethiol heads connecting the molecules to the surface) types, self-assembling on a spherical geometry. The isotropic interactions represents effective interactions between alkanethiol molecules and the reach of the molecules is the cause for the long range of the interaction potential. For a fixed stoichiometry of surface types, different parts of the ground state configuration coincides with different minima of the energy spectrum, allowing us to extract more information (as opposed to just one length scale the one component systems are defined by) from the energy spectrum as well as making a larger morphological space available. Paper V describes how to predict the composition of stripes and spots that self-assembles from the effective interactions among the surface molecules. Paper VI uses the connection between energy spectrum and ground state configuration to design functional self-assembled surface pattern, with patches oriented in a way that causes the coated nano-particles themselves to self-assemble into different geometric structures.

As a final note I explore another self-assembling system, a two-dimensional model organism with a few distinct cell types where cell division is governed by the immediate surrounding of the cell. Just like how we started out with the self-assembling particle systems, the first step have been to explore what type of patterns that can emerge from the model mechanisms, and explain those patterns. Unlike the particle system there is no universal cell patterns that emerge from wide ranges of cell behaviour, the model has a rich morphological space. In the draft paper in the Appendix, I focus on a few distinct functional patters: shells, protrusions and cell interweaving as they can be considered building blocks for more complicated cell structures. The mechanism behind shell growth for example, is in this model when the cells beneath the shell divide as a consequence of their immediate vicinity to the shell. In turn, the cells of the shell divide when the shell is stretched thin, increasing the interface towards the enclosed cells as well as the exterior. The growth of the shell is self-regulated.

Initially the our design principles required very complicated interactions, far removed from what is realistic for micro- and nano-scale systems. But gradually we have bridged the gap between theory and experiments, with principles for how to simplify the designed interaction potentials and the alkanethiol on gold model that while not an exact representation is no more complex than its real world counterpart. We are currently collaborating with experimentalists on sedimenting silica particles, where the goal is to develop a framework for testing and verifying our approach to designed self-assembly against experiments.

The cell model in the draft paper in the Appendix is also an abstraction of how real cells behave. Now that I know how to link growth criteria with emerging cell structures, the next step is to make the growth criteria more realistic, for example by linking it to gene regulatory networks. Interestingly, the reaction diffusion that describes gene regulatory networks is another example where Fourier analysis is can be used to describe and explain emerging patterns. I hope that eventually, our work on designed self-assembly in particle systems will be a foundation for designing hierarchical self-assembly of cell structures. This hierarchy would consist of a gene regulatory network designed to activate cell growth in cells in specific situations, which in turn would make the organism grow to desired shapes.

Bibliography

1. Nam, K. T., Wartena, R., Yoo, P. J., Liau, F. W., Lee, Y. J., Chiang, Y.-M., Hammond, P. T. & Belcher, A. M. Stamped microbattery electrodes based on self-assembled M13 viruses. *Proceedings of the National Academy of Sciences* **105,** 17227–17231 (2008).
2. Ozin, G. A. & Yang, S. M. The Race for the Photonic Chip: Colloidal Crystal Assembly in Silicon Wafers. *Advanced Functional Materials* **11,** 95–104 (2001).
3. Smith, D. R., Pendry, J. B. & Wiltshire, M. C. K. Metamaterials and Negative Refractive Index. *Science* **305,** 788–792 (2004).
4. Shelby, R. A., Smith, D. R. & Schultz, S. Experimental Verification of a Negative Index of Refraction. *Science* **292,** 77–79 (2001).
5. Douglas, S. M., Dietz, H., Liedl, T., Hogberg, B., Graf, F. & Shih, W. M. Self-assembly of DNA into nanoscale three-dimensional shapes. *Nature* **459,** 414–418 (May 2009).
6. Chen, Q., Bae, S. C. & Granick, S. Directed self-assembly of a colloidal kagome lattice. *Nature* **469,** 381–384 (2011).
7. Engel, M. & Trebin, H. Self-Assembly of Monatomic Complex Crystals and Quasicrystals with a Double-Well Interaction Potential. *Physical Review Letters* **98,** 225505 (2007).
8. Marjorie J., V. The effect of adsorption on the van der waals interaction of spherical colloidal particles. *Journal of Colloid Science* **16,** 1–12 (1961).

9. Louis, A. A., Allahyarov, E., Löwen, H. & Roth, R. Effective forces in colloidal mixtures: From depletion attraction to accumulation repulsion. *Physical Review E* **65,** 061407 (2002).
10. Currie, E., Norde, W. & Cohen Stuart, M. Tethered polymer chains: surface chemistry and their impact on colloidal and surface properties. *Advances in Colloid and Interface Science* **100–102,** 205–265 (2003).
11. Edlund, E. & Jacobi, M. N. Universality of Striped Morphologies. *Physical Review Letters* **105,** 137203 (2010).
12. Torquato, S. Inverse optimization techniques for targeted self-assembly. *Soft Matter* **5,** 1157 (2009).
13. Rothemund, P. W. K. Folding DNA to create nanoscale shapes and patterns. *Nature* **440,** 297–302 (2006).
14. Locke, M. The Cuticular Pattern in an Insect, Rhodnius Prolixus Stål. *Journal of Experimental Biology* **36,** 459–477 (1959).
15. Handberg-Thorsager, M., Fernandez, E. & Salo, E. Stem cells and regeneration in planarians. *Frontiers in bioscience : a journal and virtual library* **13,** 6374–6394 (2008).
16. Gardner, C. & Radin, C. The infinite-volume ground state of the Lennard-Jones potential. English. *Journal of Statistical Physics* **20,** 719–724 (1979).
17. Torquato, S. Inverse optimization techniques for targeted self-assembly. *Soft Matter* **5,** 1157–1173 (6 2009).
18. Folland, G. & Sitaram, A. The uncertainty principle: A mathematical survey. English. *Journal of Fourier Analysis and Applications* **3,** 207–238 (1997).
19. Grivopoulos, S. Stem cells and regeneration in planarians. *Journal of Physics A: Mathematical and Theoretical* **42,** 115–212 (2009).
20. Gayathri, V. S. & Rao, M. Fluctuation-induced chiral symmetry breaking in autocatalytic reaction-diffusion systems. *Europhysics Letters (EPL)* **80,** 28001 (2007).
21. Katano, S., Kim, Y., Matsubara, H., Kitagawa, T. & Kawai, M. Hierarchical Chiral Framework Based on a Rigid Adamantane Tripod on Au(111). *J. Am. Chem. Soc.* **129,** 2511–2515 (2007).
22. Cao, Z., Gu, N. & Gong, F.-C. Stripe domain analysis of alkanethiol and alkynethiol monolayers self-assembled on the surfaces of gold grains. *Materials Science and Engineering: C* **27,** 773 –780 (2007).

23. Zhang & Glotzer, S. C. Self-Assembly of Patchy Particles. *Nano Letters* **4,** 1407–1413 (2004).
24. Yi, G.-R., Pine, D. J. & Sacanna, S. Recent progress on patchy colloids and their self-assembly. *Journal of Physics: Condensed Matter* **25,** 193101 (2013).
25. Wang, Y., Wang, Y., Breed, D. R., Manoharan, V. N., Feng, L., Hollingsworth, A. D., Weck, M. & Pine, D. J. Colloids with valence and specific directional bonding. *Nature* **491,** 51–55 (2012).
26. Boncheva, M. & Whitesides, G. M. Making Things by Self-Assembly. *MRS Bulletin* **30,** 736–742 (10 2005).
27. Williams, D., Van Frank, R., Muth, W. & Burnett, J. Cytoplasmic inclusion bodies in Escherichia coli producing biosynthetic human insulin proteins. *Science* **215,** 687–689 (1982).
28. Gee, H. Biomechanics: Gripping feat. *Nature* **405,** 631–631 (2000).
29. Lafuma, A. & Quere, D. Superhydrophobic states. *Nat Mater* **2,** 457–460 (2003).
30. Bronzino, J. D. & Peterson, D. R. *Tissue engineering and artificial organs* (CRC press, 2010).
31. Ujihara, Y., Nakamura, M., Miyazaki, H. & Wada, S. Proposed Spring Network Cell Model Based on a Minimum Energy Concept. English. *Annals of Biomedical Engineering* **38,** 1530–1538 (2010).